

Clinical

Recovery of elasticity of aged human epithelial cells in vitro

Igor Sokolov, PhD,^{a,b,*} Swaminathan Iyer, PhD,^a Craig D. Woodworth, PhD^c

^aDepartment of Physics, Clarkson University, Potsdam, New York, USA

^bDepartment of Chemistry, Clarkson University, Potsdam, New York, USA

^cDepartment of Biology, Clarkson University, Potsdam, New York, USA

Received 11 July 2005; Accepted 23 December 2005

Abstract

We recently found a considerable increase in rigidity of human epithelial cells during aging in vitro. This is important because the loss in elasticity of epithelial tissues with aging contributes to many human diseases. We also found that cultured cells had three distinct regions of rigidity and that the increase in rigidity correlated with an increase in density of cytoskeletal fibers. However, it was not clear which type of fiber was important. Atomic force microscopy and immunofluorescence microscopy were used in this study to characterize aging human epithelial cells in *vitro*, both before and after treatment with *cytochalasin B*. We found that the fibers associated with increased rigidity were mostly F-actin microfilaments. Furthermore, using cytochalasin B, a chemical that inhibits polymerization of F-actin, we restored the rigidity of old cells to the young level in all three areas of rigidity simultaneously. These results clarify how the cell mechanics changes during aging in vitro, and they may be relevant for treatment of age-related loss of elasticity in epithelial tissues.

© 2006 Elsevier Inc. All rights reserved.

Key words:

Atomic force microscopy; Scanning probe microscopy; Cytoskeleton; Aging epithelial cells; Age-related diseases; Young's modulus

The increase of rigidity of human epithelial tissues with aging [1] has been implicated in the pathogenesis of many diseases associated with aging, including vascular diseases, kidney disease, cataracts, Alzheimer's dementia [2,3], complications of diabetes, and cardiomyopathies [4]. It had been believed that the increase of tissue rigidity resulted exclusively from cross-polymerization of collagen and elastin in the extracellular matrix [1]. Many treatments [4,5] for age-related diseases are based on this belief. However, we have recently shown that epithelial cells also become considerably more rigid after aging in vitro [6]. Apart from contributing to the increased rigidity of epithelial tissue as a whole, the more rigid cells may decrease the permeability of the epithelial layer, which is important for many biological functions. Therefore, a possible decrease of rigidity would definitely be beneficial for the function of epithelial tissue.

In previous work [6] we found a positive correlation between increased cell rigidity in aged cells and the surface density of cytoskeletal fibers. To study the cytoskeleton quantitatively, we developed a new method [7] using atomic force microscopy (AFM). Although this method has a number of advantages, it cannot identify the type of cytoskeletal fibers that are imaged. In the present studies we have extended our previous work by using AFM in combination with standard immunofluorescence microscopy. This has allowed us to determine that the majority of fibers are microfilaments such as F-actin. On the basis of this observation, we now report that treatment of old cells with cytochalasin B, a chemical that inhibits polymerization of F-actin, reduces cell rigidity to levels observed in cultures of young cells. In general, this is an important finding because of the following observations. As we showed before [6], each epithelial cell has three distinctive regions of rigidity: the area above the nucleus, the cytoplasm, and the cell edge. All three areas have quite distinctive cytoskeletal content. Therefore, it is not obvious that treatment with cytochalasin B would restore the elasticity in all three areas. Fortunately, we show here that after an appropriate treatment, it is possible to reduce the rigidity of old cells to the young level in all three areas

No financial conflict of interest was reported by the authors of this paper.

* Corresponding author. Department of Physics, Clarkson University, Potsdam, NY 13699-5820 USA.

E-mail address: sokolov@clarkson.edu (I. Sokolov).

simultaneously. These results may contribute to the development of treatments to minimize the age-related loss of elasticity in epithelial tissues.

Materials and methods

Preparation of the cytoskeleton for AFM and immunofluorescent imaging

The cells that attached and grew on the Petri dish were washed twice with Hanks' Balanced Salt Solution (HBSS) and then treated overnight at 4 °C with a solution of 0.5% Triton X-100 detergent (Sigma, Ronkonkoma, NY) mixed with buffer (0.14 M NaCl, 5 mM MgCl₂) to solubilize the plasma membrane and organelles and to remove soluble cytoplasmic proteins. After this treatment the remaining cytoskeletal network was washed twice for 2 minutes in the buffer and then fixed in the buffer with 1% formalin for 10 minutes. The fixative was removed and the cells were washed twice with HBSS. A dilute solution of 10 μL methanolic stock solution of Alexa Fluor 488 phalloidin in 200 μL HBSS was used when staining for each cover slide. The cells were left overnight at 4 °C with the staining stock solution. The fixative was then removed and the cells washed twice with HBSS. The cells were washed with MilliQ ultrapure water (Millipore Corporation, Bedford, MA) and dried under ambient conditions for scanning in air and for fluorescent imaging.

It should be noted that the procedure described above is a slight modification of the method that we used previously [7]. Specifically, 10 mM M Tris-HCl was excluded from the buffer. This is because Alexa Fluor 488 phalloidin is not bound to F-actin in the presence of Tris. The AFM imaging of the extracted cytoskeleton is unchanged by exclusion of the Tris.

AFM

A Nanoscope Dimension 3100 (Digital Instruments/Veeco, Inc., Santa Barbara, CA) atomic force microscope was used in the present study. A standard cantilever holder cell for operation in liquids was used. To measure the Young's modulus, the force-volume mode of operation was used. The AFM software version used was 5.12, release 4. To image the cells, either contact or tapping mode of scanning was used. All scanning and measurements related to rigidity were performed on viable cells maintained in HBSS solution. Scanning of the cytoskeleton was performed in ambient conditions.

AFM probe preparations

A V-shaped standard narrow 200-μm AFM cantilever (Digital Instruments/Veeco, Santa Barbara, CA) was used throughout the study. Whereas for cytoskeleton imaging the cantilever was used as is, for measurement of rigidity the AFM probe was modified as follows. A 5-μm-diameter silica

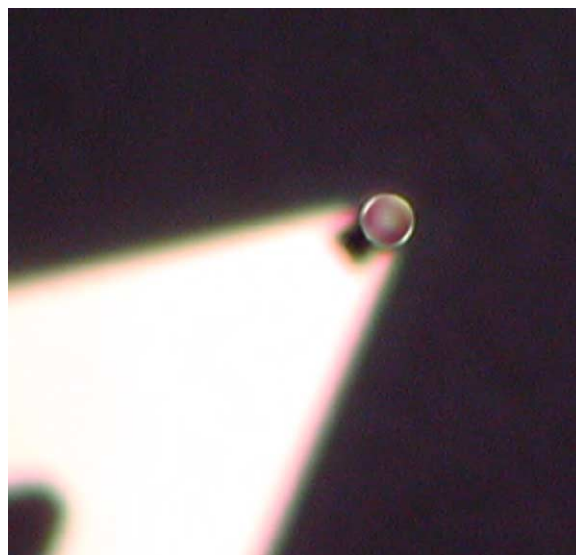


Fig 1. A 5-μm silica sphere glued to a standard AFM cantilever was used to obtain stable and reproducible results over the area of an individual cell.

ball was glued to the cantilever with epoxy resin using the AFM built-in micromanipulator. Such a modified probe was an essential part in this study for the following three reasons: First, this probe has a considerably larger area of contact with the cell than does a typical commercial probe (radius of curvature ~5–50 nm) commonly used for such measurements. The larger area of probe-cell contact results in averaging local variation in rigidity compared with that measured with the regular sharp probe. This leads to less variation of the Young's modulus. Thus we needed fewer measurements to gather good statistics. This was very important because of the limited time (~2 hours) of the measurements when the cells were viable in the HBSS solution. Second, the low rigidity at the edge of the cell would make it very difficult, if not impossible, to make measurements with a sharp AFM tip. The sharp tip simply penetrates the thin areas of the cell and indicates an even higher rigidity because of its contact with the rigid substrate. Third, using the 5-μm probes caused much less damage to the cell during the scanning.

After each series of measurements the probe was changed. In some cases it was possible to clean it in acid/base solutions. The radius of the probe and its cleanliness were tested by scanning the reversed grid (TGT1, NT-NDT, Inc., Russia). The result of gluing and positioning of the silica sphere can be easily checked with the regular optical microscope as shown in Figure 1. The cantilever spring constant was measured using the built-in option of the Nanoscope software.

Fluorescent microscopy

A Nikon Eclipse TE200 inverted microscope was used for immunofluorescent measurements of the cells prepared

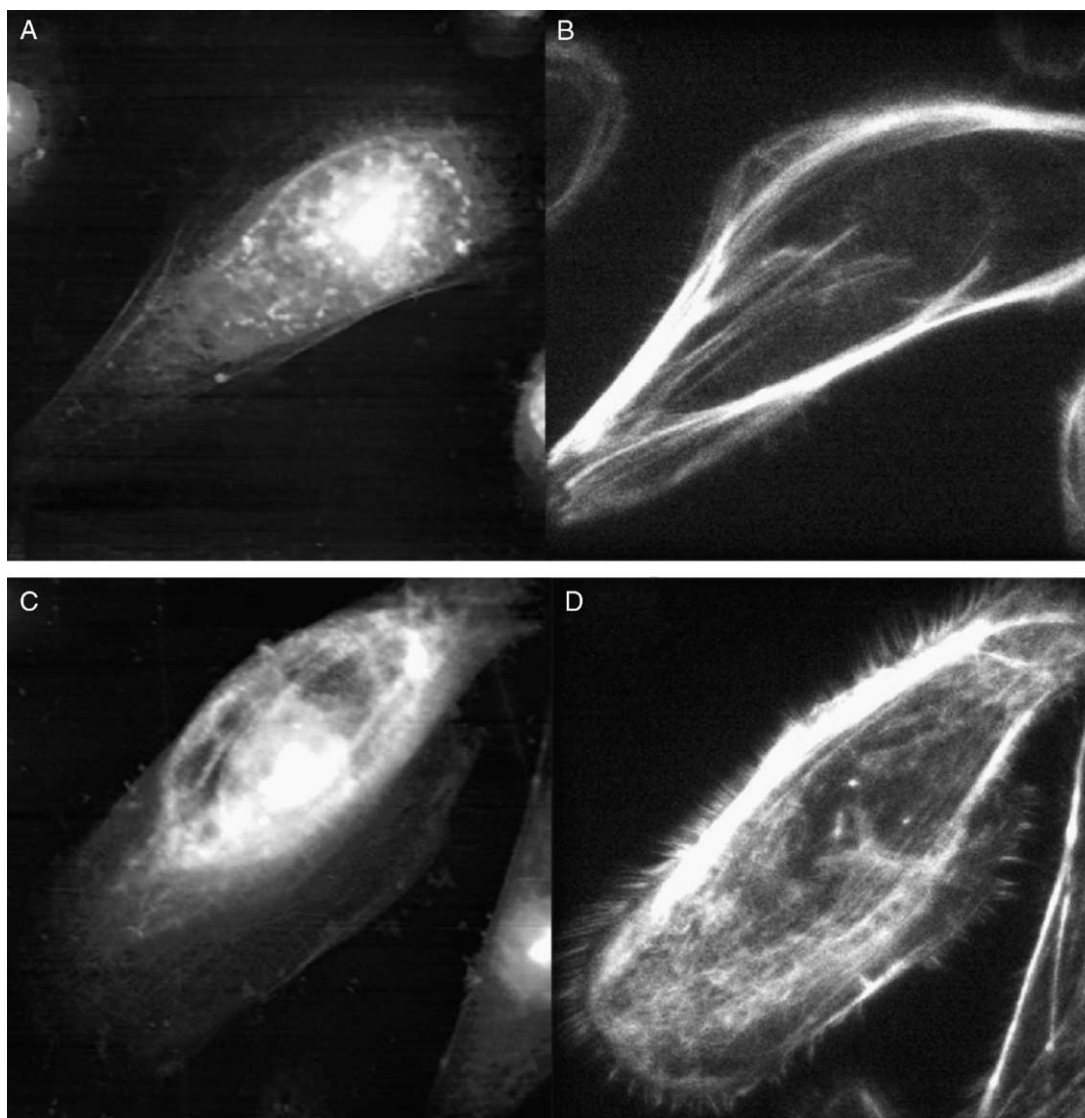


Fig 2. Complementary fluorescence images (B, D) and AFM height images (A, C) of the same cells. Lateral size (A, C): $100 \times 100 \mu\text{m}^2$.

as described above. A 100-W Mercury source (CHIU Technical Corporation, Kings Park, New York) was used to illuminate the sample. An FITC 31001 filter (Chroma Technology Corporation, Rockingham, VT) for fluorescent mercury lamp excitation was used. Simple PCI Automated Image Capture software: Image Pro Express was used to capture images using an ORCA Hamamatsu CCD camera (Media Cybernetics, Inc., Silver Spring, MD).

Cell culture and cytochalasin B treatment

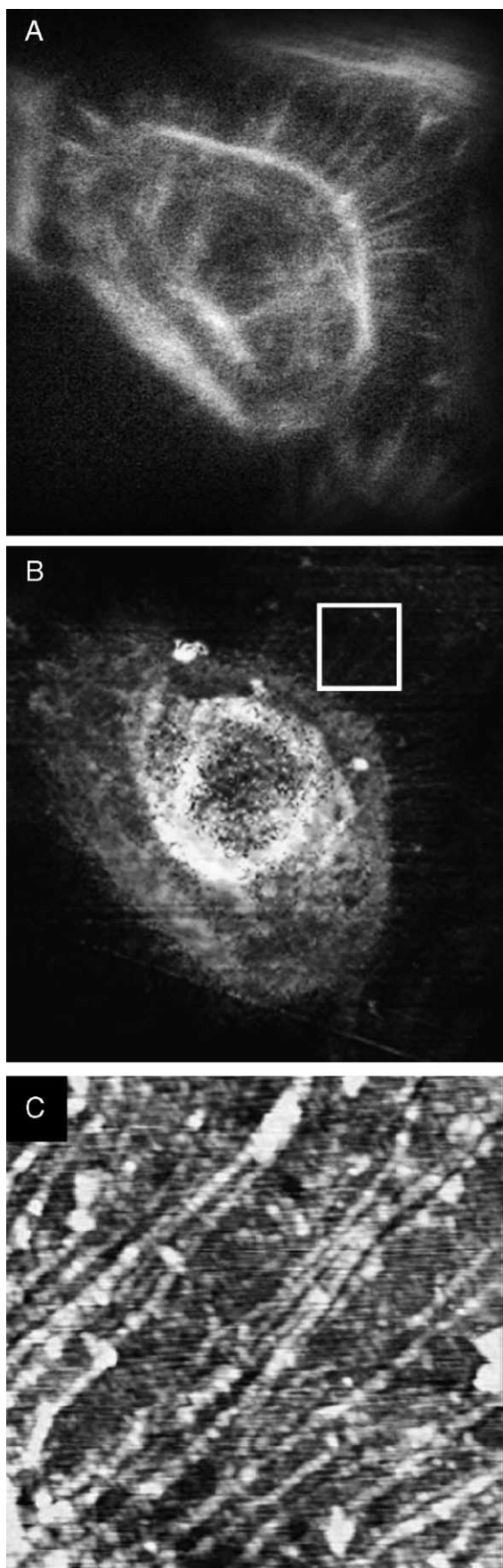
Primary cultures of human foreskin epithelial cells were prepared by a two-stage enzymatic digestion as described [8], and cells were maintained in keratinocyte serum-free medium (Invitrogen, Carlsbad, CA). Young cultures typically consisted of cells that had been maintained for fewer than 3 passages in vitro (<25 population doublings). Old, in vitro-aged cell cultures were maintained between 8 and 12 passages (>50 population doublings). The epithelial cells

adhered tightly to the bottom of the plastic dish, and the 60-mm cell culture dishes were mounted on the chuck of the AFM with a double sticky tape.

Old cells were treated with cytochalasin B (Sigma Aldrich, St. Louis, MO), a cell-permeable fungal toxin that binds to the barbed end of actin filaments inhibiting both the association and dissociation of its subunits. A $4 \mu\text{g}/\text{mL}$ solution of cytochalasin B in the medium was used to treat viable cells for 12 hours. It should be noted that we used the same aged cells (from the same source) in this work as in our previously published study [6].

Cell rigidity measurements

Cells prepared as described in the previous section were washed twice with the HBSS buffer solution and consequently imaged in that buffer at room temperature. In each experiment the AFM cantilever sensitivity was calibrated against a rigid substrate, a small piece of silicon



wafer immersed in the HBSS solution in the Petri dish. The duration of each experiment was no longer than 2.5 hours to ensure viability of the cells. As we demonstrated before [6], the cell rigidity is not changed within its variation on the cell during this time. The details of the measurements of the cell rigidity are described in our previous work [6]. Below we briefly outline a few important points.

To find the rigidity, which is characterized by the Young's modulus, we used the force-volume mode of the AFM operation. This is important because we need to know of topography and the force-distance curves at each point simultaneously. The force curves were collected over areas of $20 \times 20 \mu\text{m}^2$ with the height change within $7 \mu\text{m}$ (Z limit of the scanner). The global position of the AFM scan was controlled by the built-in video system, which allows observation of areas from $150 \times 110 \mu\text{m}^2$ to $675 \times 510 \mu\text{m}^2$ with $1.5\text{-}\mu\text{m}$ resolution.

To process the data we used the Hertz-Sneddon model [9] because of the relatively low adhesion between the AFM probe, a clean silica sphere, and the cell. It is important to stress the applicability of these models to our cell system. Obviously, the cell is not a homogeneous medium. However, as has been shown in the literature [10–13], the approximation of a homogeneous medium that is used in the Hertz-Sneddon model works quite well in the description of the mechanical properties of cells. It was, however, expected and observed that the Young's modulus changed when the probe penetrated too far into the cell. Therefore, here we consider the Young's moduli for penetrations no deeper than $\sim 100 \text{ nm}$.

Results and discussion

Comparative study of cytoskeleton: AFM and immunofluorescent imaging

We previously reported a correlation between the density of the cytoskeleton and cell rigidity in aging epithelial cells [6]. In that study the cytoskeleton was imaged with the AFM. Although this method provides quantitative and quite precise information about the cytoskeleton, it cannot differentiate between fibers of different nature. To identify which types of fibers we observed with the AFM, we used immunofluorescence labeling of F-actin, the material of microfilaments. The choice of F-actin labeling was based on the results of previous research. Early work on the cytoskeleton of human peripheral blood lymphocytes showed that the concentration of F-actin fibers increases in older cells

Fig 3. **A**, Fluorescence $50 \times 50 \mu\text{m}^2$ image, and **B**, AFM $40 \times 40 \mu\text{m}^2$ height image of the same cell. **C**, High-resolution AFM height image: $6.7 \times 6.7 \mu\text{m}^2$ of the individual actin filaments outside the cell. Area shown is highlighted in **B** by a white rectangle.

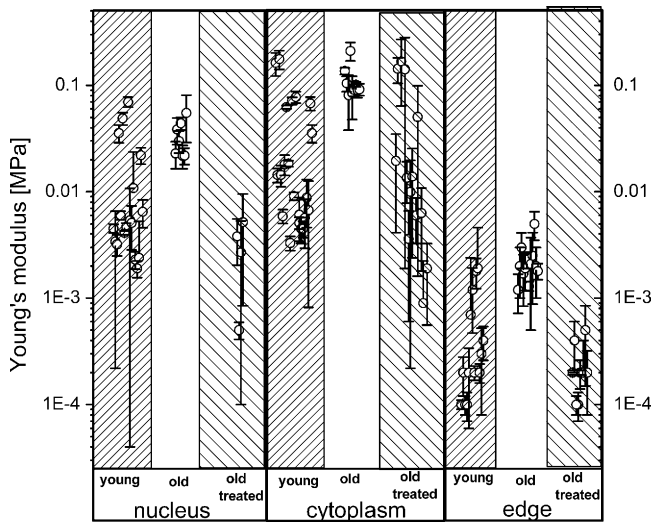


Fig 4. Results of the rigidity measurements grouped for the nucleus, cytoplasm, and edge areas of the young, old, and treated old cells. The data for the young and old untreated cells are taken from our previous work [6] and shown here for comparison.

[14]. Recent work on the measurement of rigidity of rat liver macrophages [10] and transformed mouse fibroblasts [11] using AFM demonstrated that actin fibers have a considerable influence on cell rigidity.

To correlate the AFM images of the cytoskeleton (prepared as described above) and the fluorescent images, we applied both methods to the same cells. Using immunofluorescence labeling we obtained images of microfilaments (F-actin) and compared those images to the AFM scans of the same areas. A few representative images of the same cells obtained by both AFM and fluorescence microscopy are presented in Figure 2. To compare the fluorescent and AFM images, it is important to remember that the contrast in both cases comes from different sources. Whereas the fluorescent signal is proportional to the number of fluorescent molecules attached to F-actin, the AFM contrast is proportional to the physical height of molecules of the cytoskeleton at each point on the surface. Therefore, we cannot expect to see the same images of the cells in both techniques. The cell treatment used in this work may destroy the cytoskeletal fibers and, on the other hand, do not remove all noncytoskeletal proteins. All these variables could alter the physical appearance of the cells imaged with AFM, whereas they may still produce a fluorescent signal. Therefore, on comparing AFM and fluorescent images we can expect to see at best a positive correlation between the physical presence of molecules and fluorescent signal. Comparing these in Figure 2, one can see a good correlation between fluorescence (Figure 2, B, D) and AFM images in height mode (Figure 2, A, C). The only large difference is seen in the nuclear region. This can easily be explained by recalling that the nuclei were not removed by our treatment,

and AFM shows nuclear regions as bright spots. Indeed, that was the reason we could draw conclusions about a correlation between rigidity and cytoskeleton in the cytoplasmic and edge areas of the cell, but not for the nuclear regions [6].

Because small height features are hardly seen in the AFM height images, Figure 3 demonstrates that F-actin fibers surrounding the cells can also be seen in the AFM image. As before, the fluorescent image (Figure 3, A), shows clearly the surrounding fibers, whereas the AFM scan (Figure 3, B) does not. However, bunches of actin filaments are clearly visible in an enlarged area shown in Figure 3, C (highlighted in Figure 3, B by a white rectangle. The minimal vertical size of the filaments lying on a flat substrate near the cells was around 8 to 11 nm, which is close to the expected actin filament diameter of 6 to 10 nm.

To summarize, based on these results we conclude that the AFM images are well correlated with the presence of microfilaments (F-actin) outside the nuclear region. Therefore, the observed connection between the rigidity and density of cytoskeletal fibers is the connection between rigidity and the density of microfilaments, F-actin. This justifies our decision to proceed with the treatment (described in Materials and Methods) that leads to the decrease of the amount of F-actin inside cells. In the next section we show that the treatment indeed results in the decrease of rigidity.

Decrease of rigidity of old cells after the treatment with cytochalasin B

To obtain statistically meaningful results we measured the rigidity of 15 treated old cells. Each cell was measured in all three regions of rigidity. It should be noted that because of difficulties of scanning such soft objects as cells, not all measurements were successful. Because the height of a cell was larger than the range of the AFM scanner, we had to re-engage the atomic force microscope for almost every measurement to accommodate the entire range of cell heights. That is why the number of successful measurements is slightly different for different regions.

Figure 4 shows the results of measurements of the Young's modulus for old cells after treatment. For comparison we included the values of the Young's moduli for the young and old cells that were not treated with cytochalasin B. Those results are taken from our previous work [6]. Following notation of that work, each point on the plot stands for an average of 30 to 100 moduli that were calculated over the area up to $20 \times 20 \mu\text{m}^2$. The exact number of the analyzed moduli was determined by overall deviation the imaged cell surface from flat. This is because we used the sphere–flat surface model for calculation of the Young's modulus. Therefore, we calculated the Young's modulus only over relatively flat areas of the cells ($<10\text{--}15$ deg of inclination angle). The "error" bar reflects the variability, one standard deviation from the average.

One more note concerns the variation of the Young's modulus for young cells. As can be seen in Figure 4, the modulus distribution for young cells is somewhat bipolar. Many measurements for young cells were centered around the median values for rigidity of the old cells. This effect might occur if there was ambiguity in defining the age of the young cells. Such an effect might be expected because some epithelial cells age more rapidly than others, as described for human skin [15–17]. Thus a certain percentage of cells might have characteristics intermediate between young and old cells. If we consider the “softer” distribution as a true young cell rigidity, young cells will have the following average moduli: approximately 5 kPa (nucleus), approximately 7 kPa (cytoplasm), and approximately 0.2 kPa (edge). Comparing these values with the moduli measured for old treated cells, one can see that old cells became as soft as about 3 kPa (down from 33 kPa for the nucleus area), about 5 kPa (down from 110 kPa for the cytoplasmic area), and about 0.2 kPa (down from 2.2 kPa for the edge). Thus the decrease in rigidity is equal to 11, 22, and 11 times for the nucleus, cytoplasm, and edge areas, respectively. It can be seen that the rigidity of all three regions was restored to levels very close to those of young cells. This is a notable result, because the cytoskeletal contents vary considerably in each of these three areas of rigidity.

It is worth noting the longevity of the treated cells. Cytochalasin B acts not as a destroyer but inhibitor of polymerization of F-actin by shifting the balance between polymerization and depolymerization. Therefore, we expect long-time survival of the treated cells. Nevertheless, additional experiments are needed to clarify this issue.

In conclusion, using immunofluorescence microscopy we found that our previously developed technique for studying the cytoskeleton by AFM revealed mostly microfilaments. Therefore, our previously observed correlation between cell rigidity and density of the cytoskeleton is mostly a correlation between the cell rigidity and density of microfilaments. In other words, old cells are more rigid and have denser microfilaments. With this observation in mind we treated old cells with cytochalasin B, a cell-permeable fungal toxin that binds to the barbed end of actin filaments, inhibiting polymerization. As a result, the rigidity of the old cells decreased to the level found in young cells. As described previously, each cell has three distinctive areas of rigidity: nucleus, cytoplasm, and edge. Because the cytoskeletal contents differ in each area, we did not actually expect the desired amount of decrease to the young level in all three areas simultaneously. Fortunately, the treatment succeeded in accomplishing just that. The amount of rigidity decrease was equal to 11, 22, and 11 times for the nucleus, cytoplasm, and edge areas, respectively. Thus the final rigidity of treated old cells was rather close to the young cells. This discovery may have relevance for the treatment and prophylaxis of

age-related diseases that are caused by loss of elasticity of epithelial tissues.

Acknowledgment

This material is based upon work partially supported by Wallace H. Coulter Foundation, the NSF under Grant CCR-0304143 and by NYSTAR (CAMP-33378). The authors are thankful to Prof. Edward Moczydlowski for letting us using his fluorescent microscope.

References

- [1] Dimri GP, Lee X, Basile G, Acosta M, Scott G, Roskelley C, et al. A biomarker that identifies senescent human cells in culture and in aging skin in vivo. *Proc Natl Acad Sci U S A* 1995;92:9363–7.
- [2] Ulrich P, Zhang X. Pharmacological reversal of advanced glycation end-product-mediated protein crosslinking. *Diabetologia* 1997;40: S157–9.
- [3] Perry G, Smith MA. Active glycation in neurofibrillary pathology of Alzheimer's disease: N-(carboxymethyl) lysine and hexitol-lysine. *Free Radical Biol Med* 2001;31:175–80.
- [4] Bucala R, Cerami A. Advanced glycosylation: chemistry, biology, and implications for diabetes and aging. *Adv Pharmacol* 1992;23:1–34.
- [5] Vasan S, Zhang X, Kapurniotu A, Bernhagen J, Teichberg S, Basgen J, et al. An agent cleaving glucose-derived protein crosslinks in vitro and in vivo. *Nature* 1996;382(6588):275–8.
- [6] Berdyeva TK, Woodworth CD, Sokolov I. Human epithelial cells increase their rigidity with ageing in vitro: direct measurements. *Phys Med Biol* 2005;50(1):81–92.
- [7] Berdyeva T, Woodworth CD, Sokolov I. Visualization of cytoskeletal elements by the atomic force microscope. *Ultramicroscopy* 2005; 102(3):189–98.
- [8] Woodworth CD, Doniger J, Dipaolo JA. Immortalization of human foreskin keratinocytes by various human papillomavirus DNAs corresponds to their association with cervical carcinoma. *J Virol* 1989;63:159–64.
- [9] Sneddon IN. The relation between load and penetration in the axisymmetric Boussinesq problem for a punch of arbitrary profile. *Int J Eng Sci* 1965;3:47–57.
- [10] Tsukruk VV, Gorbunov VV, Huang Z, Chizhik SA. Dynamic microprobing of viscoelastic polymer properties. *Polymer Int* 2000; 5:441–7.
- [11] Vinckier A, Semenza G. Measuring elasticity of biological materials by atomic force microscopy. *FEBS Lett* 1998;430(1–2):12–6.
- [12] Rotsch C, Braet F, Wisse E, Radmacher M. AFM imaging and elasticity measurements on living rat liver macrophages. *Cell Biol Int* 1997;21:685–96.
- [13] Wu HW, Kuhn T, Moy VT. Mechanical properties of L929 cells measured by atomic force microscopy: effects of anticytoskeletal drugs and membrane crosslinking. *Scanning* 1998;20:389–97.
- [14] Radmacher M. Review of AFM mechanical properties of the cells. Measuring the elastic properties of biological samples with the AFM. *IEEE Eng Med Biol Mag* 1997;16:47–57.
- [15] Matzke R, Jacobson K, Radmacher M. Direct, high-resolution measurement of furrow stiffening during division of adherent cells. *Nat Cell Biol* 2001;3:607–10.
- [16] Rao KMK, Currie MS, Padmanabhan J, Cohen HJ. Age-related changes in actin cytoskeleton and receptor expression in human leukocytes. *J Gerontol* 1992;47:37–44.
- [17] Barrandon Y, Green H. Three clonal types of keratinocyte with different capacities for multiplication. *Proc Natl Acad Sci USA* 1987;84(8):2302–6.